

Gravity Inversion of the Gongola Basin Fault Structures Using the Step Model

© E. E. Epuh¹, P. C. Nwilo¹, D. O. Olorode², C. U. Ezeigbo¹, 2012

¹Department of Surveying and Geoinformatics, University of Lagos, Nigeria

²Physics Department, University of Lagos, Nigeria

Received 4 April 2011

Presented by Editorial Board Member O. M. Rusakov

Разломным структурам часто свойственны аномалии силы тяжести ступенчатого вида. Следовательно, анализ аномалий силы тяжести ввиду таких структур эквивалентен определению четырех параметров разлома: глубины от поверхности, мощности осадков, перепадам плотности и углу падения разлома. В данном исследовании выполнена инверсия силы тяжести с помощью ступенчатой модели с целью одновременной оценки четырех параметров нарушенного пласта. Модель предполагает конфигурацию, в которой бассейн заполнен однородными осадками. Для оценки параметров разлома были приняты три характеристические кривые.

Согласно анализу остаточных аномалий в пределах разломных структур глубина заложения последних не зависит от их простираения. По оценке глубины от поверхности и мощности осадков определена глубина залегания фундамента. Она не превышает 1 км в юго-западной и 7 км в северо-восточной части изучаемой области. Найденная глубина залегания фундамента соответствует приемлемой геологической модели и согласуется с материалами сейсмических и буровых работ. Материалы интерпретации использованы при построении карт изменения плотности, а также плотности кристаллических пород бассейна. Это способствовало разделению бассейна на зоны осадков, комплексы пород фундамента и гранитного плутона.

Разломним структурам часто властиві аномалії сили тяжіння східчастого вигляду. Отже, аналіз аномалій сили тяжіння з урахуванням таких структур рівноцінний визначенню чотирьох параметрів розломів: глибини від поверхні, потужності відкладів, градієнта густини і кута падіння розлому. Виконано інверсію сили тяжіння із застосуванням східчастої моделі з метою одночасної оцінки чотирьох параметрів порушеного шару. Модель припускає таку конфігурацію, коли басейн складений однорідними відкладами. Для оцінки параметрів взято три характеристичні криві.

Згідно з аналізом залишкових аномалій у межах розломних структур глибина залягання останніх не залежить від їх простягання. За оцінкою глибини від поверхні та потужності відкладів визначено глибину залягання фундаменту. Вона не перевищує 1 км у південно-західній частині та 7 км у північно-східній частині досліджуваної площі. Оцінка глибини залягання фундаменту дала правдоподібну геологічну модель, яка підтверджується матеріалами сейсмічних та свердловинних робіт. Матеріали інтерпретації використано для побудови карт змін густини, а також густини кристалічних порід басейну. Це дало змогу поділити басейн на зони осадових порід, комплекси фундаменту та гранітного плутону.

Gravity anomalies with step-like appearance are often attributed to fault structures. Analysis of gravity anomalies due to such structures is then tantamount to solving the four fault parameters: depth to the surface, sediment thickness, density contrast and the fault dip. In this research, a gravity inversion using the step model was carried out to simultaneously estimate the four parameters of the faulted bed. The model assumes a configuration that the basin is filled with homogeneous sediments. Three characteristic curves were adopted for estimating the fault parameters.

Analysis of the residual anomaly profiles of the fault structures showed that the fault structures were independent of the strike length. The estimated depth to the surface and the sediment thickness yielded the basement depth. The basement depth obtained from the gravity profiles showed a maximum basement depth of 1.0 km in the south-western part, and 7.0 km in the north-eastern part of the project area. The estimated basement depth yielded plausible geological model that corroborates with depth obtained using seismic and well information. The computed density contrast was used in the determination of density contrast and rock density maps of the basin. This helped in defining the basin into zones of sedimentary, basement complex and granite pluton.

Introduction. This model is customarily used to represent a fault for the purpose of direct analysis. From Fig. 1 the anomalous material has the form of a flat step which goes to infinity in the positive direction of x and is assumed to have a uniform density contrast throughout its entire bulk. Since most faults have a strike length that is many times their throw, the step is assumed to be two-dimensional. The model is characterized by three parameters: the density contrast $\Delta\rho$, the dip angle d , the depth to the vertical displacement ratio h/l where h , is the limiting depth and l the sediment thickness. The density contrast is as a result of the contrast between the overburden layer and the bedrock housing the mineral. Density contrast ($\Delta\rho$) is obtained by determining the upper and lower bounds on S_{\max} (Fig. 2) and calculating the

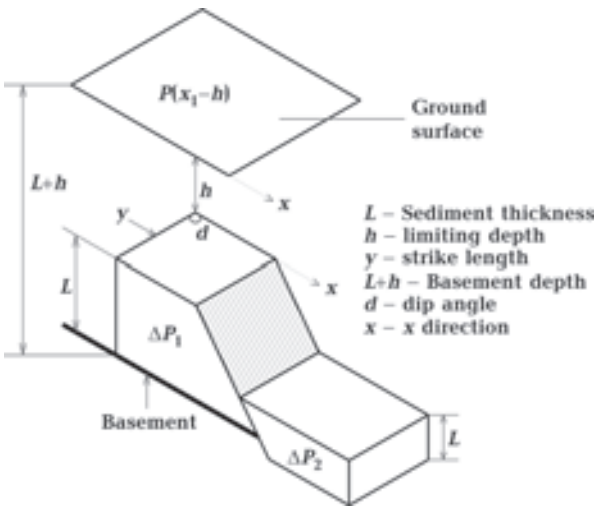


Fig. 1. Geometry of a Faulted bed.

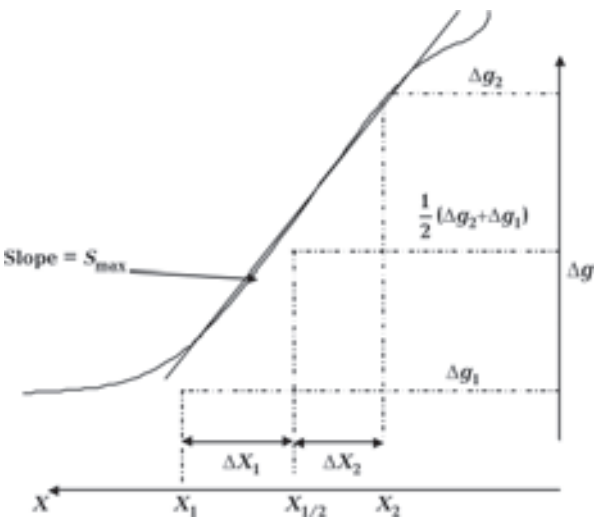


Fig. 2. Characteristic estimators for the step model [Grant, West, 1987].

density contrast using the complementary curve estimator (Fig. 3).

The Step Model Formulation. The formula for the profile of gravity effect across the step is given as follows [Grant, West, 1987]:

$$\Delta g(x) = 2G\Delta\rho \left\{ \frac{\pi}{2} + (h+l) \tan^{-1} \frac{X - \cot d}{h+l} - \tan^{-1} \frac{X}{h} + \left(X \sin^2 d + h \sin d \cos d \right) \times \ln \left[\frac{(X - \cot d)^2 + (h+l)^2}{X^2 + h^2} \right]^{1/2} - \left(X \sin d \cos d + h \cos^2 d \right) \times \left(\tan^{-1} \frac{X - \cot d}{h+l} - \tan^{-1} \frac{X}{h} \right) \right\}, \quad (1)$$

which we may write as

$$\Delta g(x) = 2G\Delta\rho f(X, h, d). \quad (2)$$

The object is to find two properties of the function $f(X, h, d)$, which may be used as estimators for h and d .

The parameters for estimating the faults using the step model are illustrated in Fig. 2.

In using the characteristic estimator in Fig. 2 the maximum horizontal gradient is measured. Then two points X_1 and X_2 are located on the profile such that the slope of the profile is equal to S_{\max} . With this, the characteristic length $X_2 - X_1$

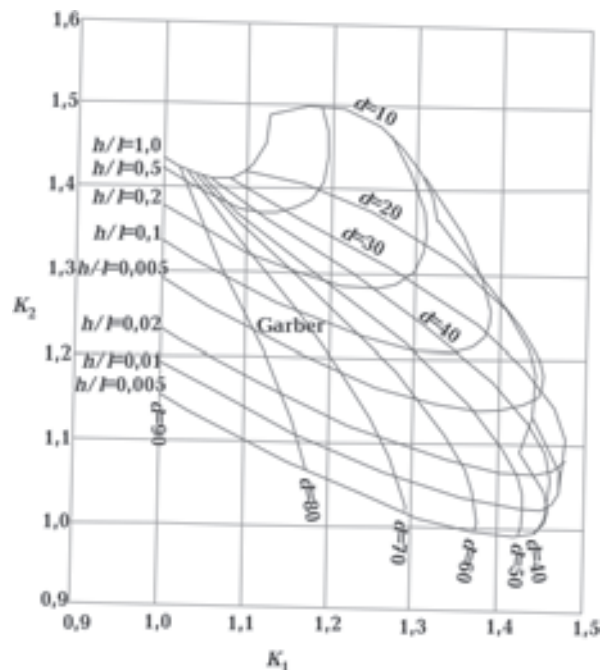


Fig. 3. Characteristics Curve, step model [Grant, West, 1987].

and a characteristic measure of amplitude $\Delta g_2 - g_1$ were obtained. It is then required to find the point $X_{1/2}$ at which the amplitude falls exactly half-way between Δg_2 and Δg_1 , and form the two ratios given as:

$$k_1 = \frac{X_2 - X_{1/2}}{X_{1/2} - X_1}, \quad (3)$$

$$k_2 = \frac{\Delta g_2 - \Delta g_1}{(X_2 - X_{1/2})S_{\max}}, \quad (4)$$

k_1 responds more to change in h than in d , while k_2 responds more strongly to change in d than in h .

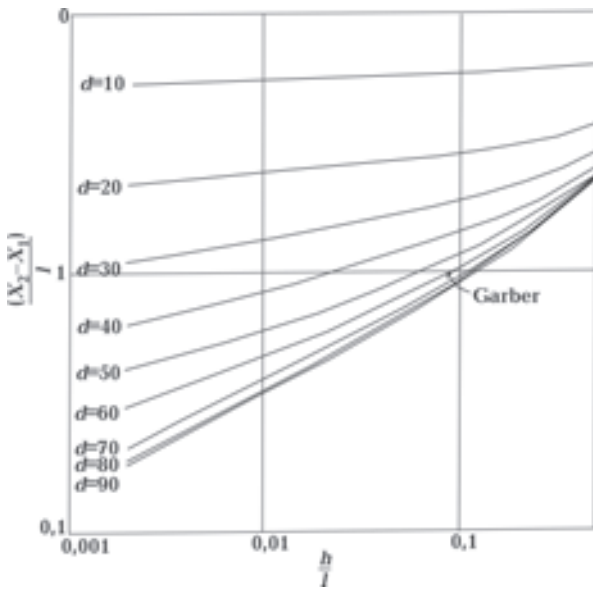


Fig. 4. Complementary curves for estimating l , step model [Grant, West, 1987].

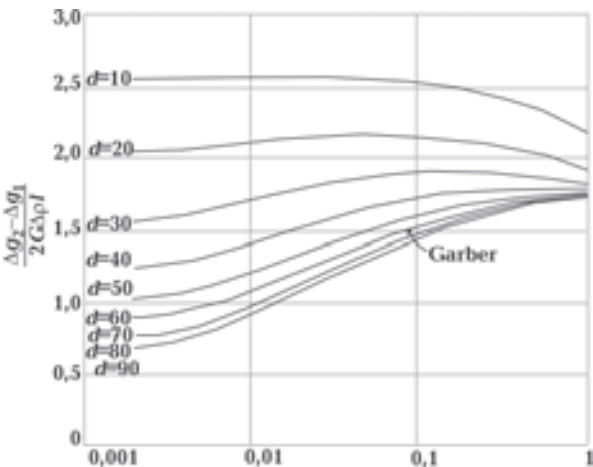


Fig. 5. Complementary curves for estimating $\Delta\rho$, step model [Grant, West, 1987].

Measurements of k_1 and k_2 on the residual gravity profile are used with the step model characteristic curves to estimate both h/l and d using Fig. 3. To separate l from h , which shows a plot of $(X_2 - X_1)/l$ versus h/l with d as parameter is used (Fig. 4). Since $(X_2 - X_1)$ can be measured and both h/l and d are known, these curves will give us l and h .

To find $\Delta\rho$, Fig. 5 is used. It shows the plot of $\frac{(\Delta g_2 - \Delta g_1)}{2G\Delta\rho l}$ versus h/l with d as parameter.

Methodology. Computation of Fault Parameters. The step model computations were carried out using equations (3) and (4) and the characteristics curves in Fig. 3—5 for the determination of fault dip D° , limiting depth $h(m)$, sediment thickness $L(m)$ and basement density contrast $\Delta\rho$. The computation for line 94D048 (Fig. 6) is stated as follows: Using equations (3) and (4) Fig. 3, we obtain $K_1=1,34$; $K_2=1,13$; $S_{\max}=0,41$; $D=55^\circ$; $h/l=0,04$, using the values of D and h/l on Fig. 4 we obtain 0,4 on the intercept. Using the values obtained Fig. 5, l is estimated as 4813 m, $h=193$ m. Using the value of D and h/l on Fig. 2, 4, we obtain the intercept of 1,1 the density contrast is computed as follows:

$$\Delta\rho = \frac{\Delta g_2 - \Delta g_1}{2G l * 1,1} = -0,139 \text{ gcc} = -0,14 \text{ gcc} .$$

In a sedimentary basin, the density contrast is always negative.

Table 1. Adopted density values for gravity modeling

Rock Type	Density, g/cm ³
Shale	2,40
Sandstone	2,61
Dolomite	2,67
Granites	2,70
Gneiss	2,75
Basic igneous	2,80

Adopted Densities for Gravity Modeling. The density values for various (sedimentary, igneous

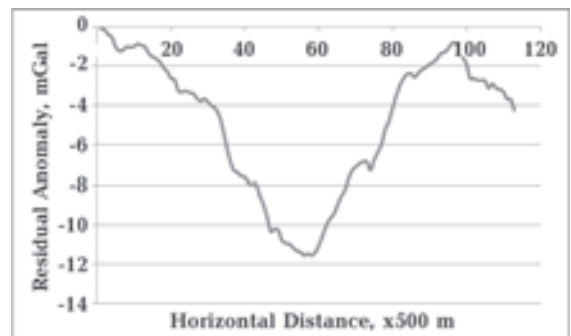


Fig. 6. Residual Gravity Anomaly Profile (94D048) Analysis.

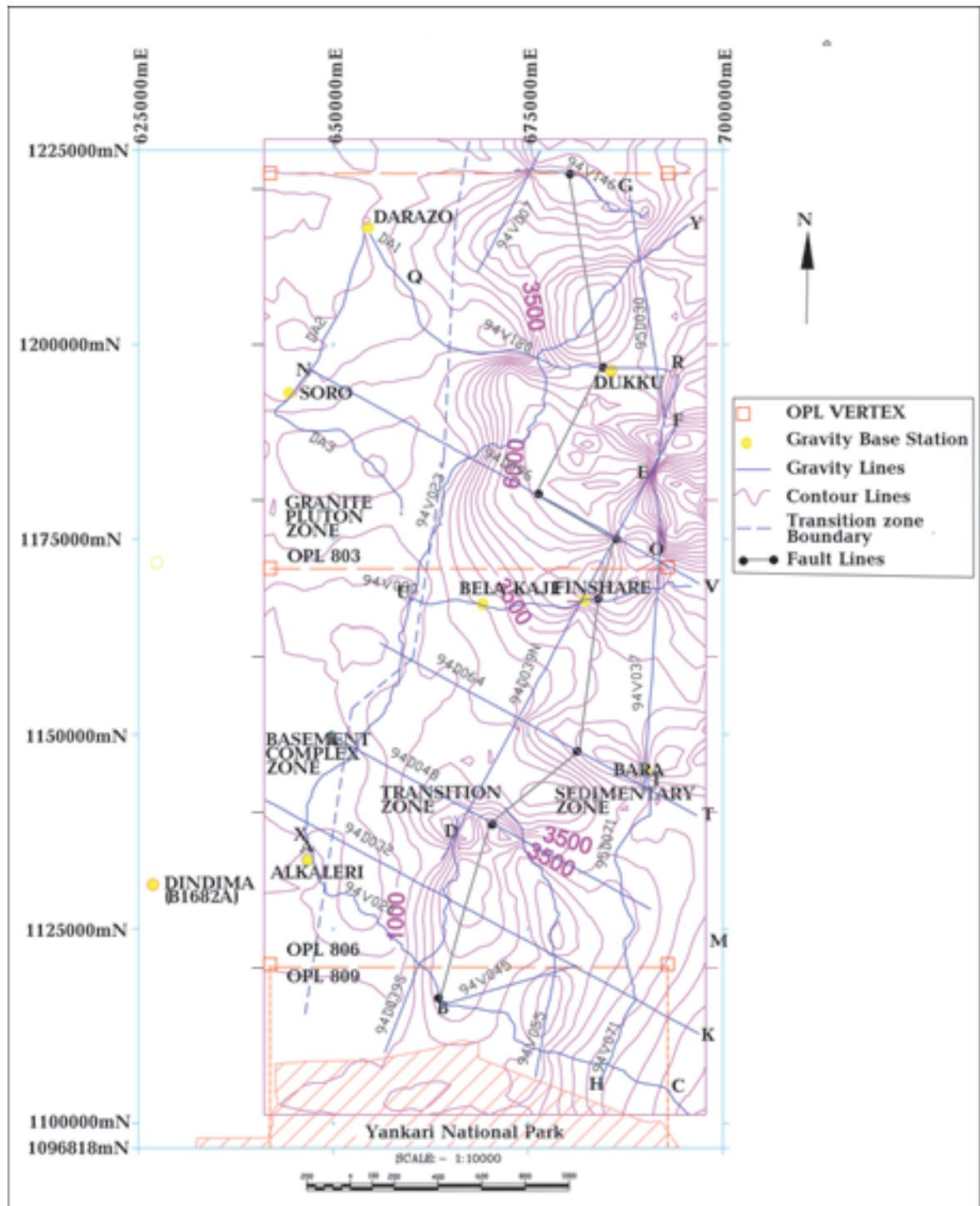


Fig. 7. Basement Depth Map (Contour Interval=500 m).

and metamorphic) rocks can be obtained from [Nettleton, 1976; Dobrin, 1988; Telford et al., 1990; Keary, Brooks, 2002]. These density values were adopted in the gravity modeling work for the identification of the rock minerals and sediments within the project area. Table 1 shows the adopted densities.

Sedimentary rocks have on the average, lower densities than igneous and metamorphic rocks. Among the sediments the average densities vary with the composition, being lowest for sandstone, followed by shale, limestone and dolomite in that order. However, actual values differ widely from the average, hence there is considerable overlap.

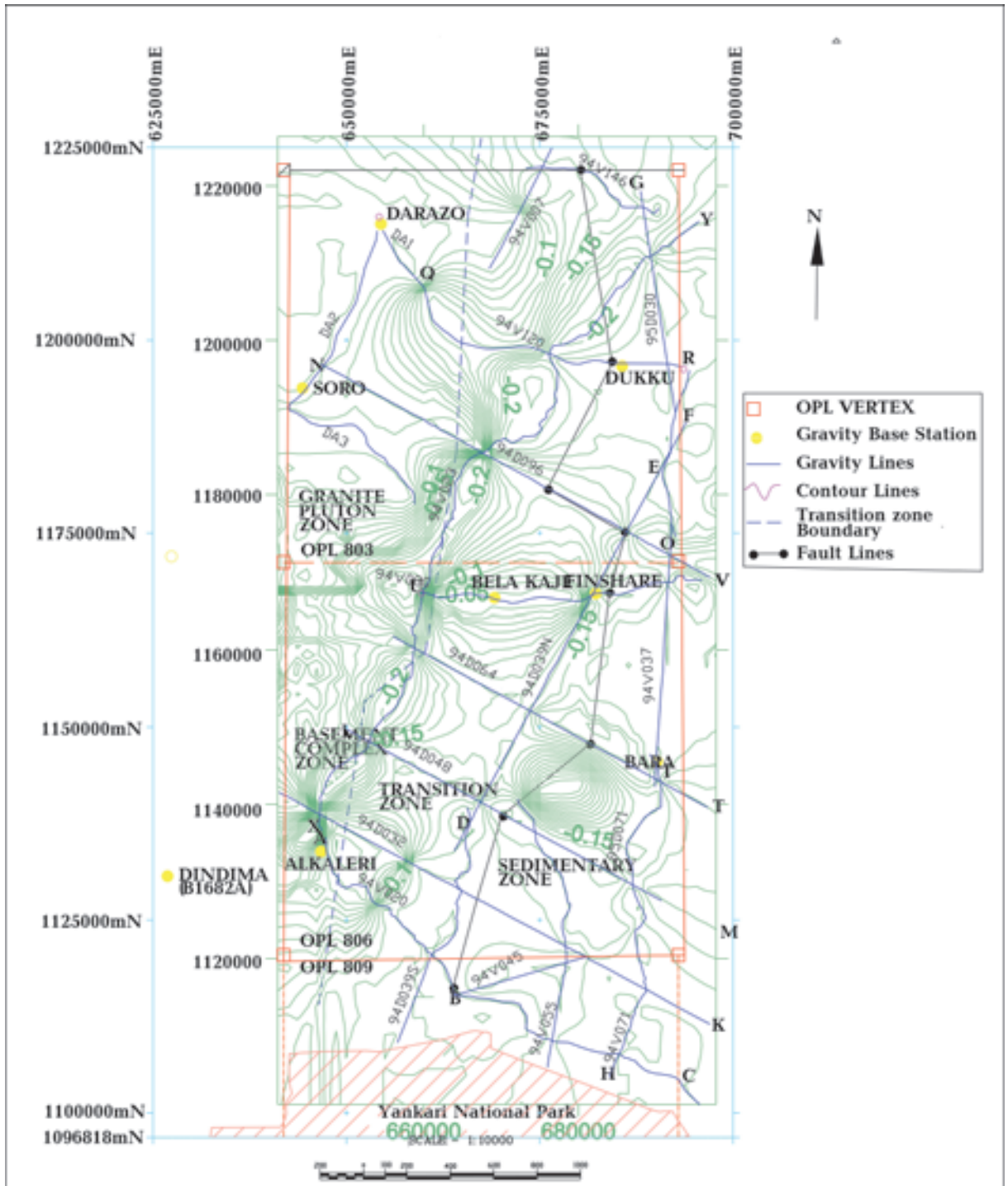


Fig. 8. Basement Density Contrast Map (Contour Interval=0,1 gcc).

Dolomites and shales are the most uniform in density.

Results and Analysis. Results. The step model computed results are shown in Tabl. 2. These include the fault dip D° , limiting depth $h(m)$, sediment thickness $L(m)$ and basement density con-

trast $\Delta\rho$. The residual gravity anomaly profiles of the lines in Tabl. 2 used in basin analysis all have a step-like appearance. The basement depth, density contrast and sediment density maps obtained from the step model results are shown in Fig. 7—11 respectively.

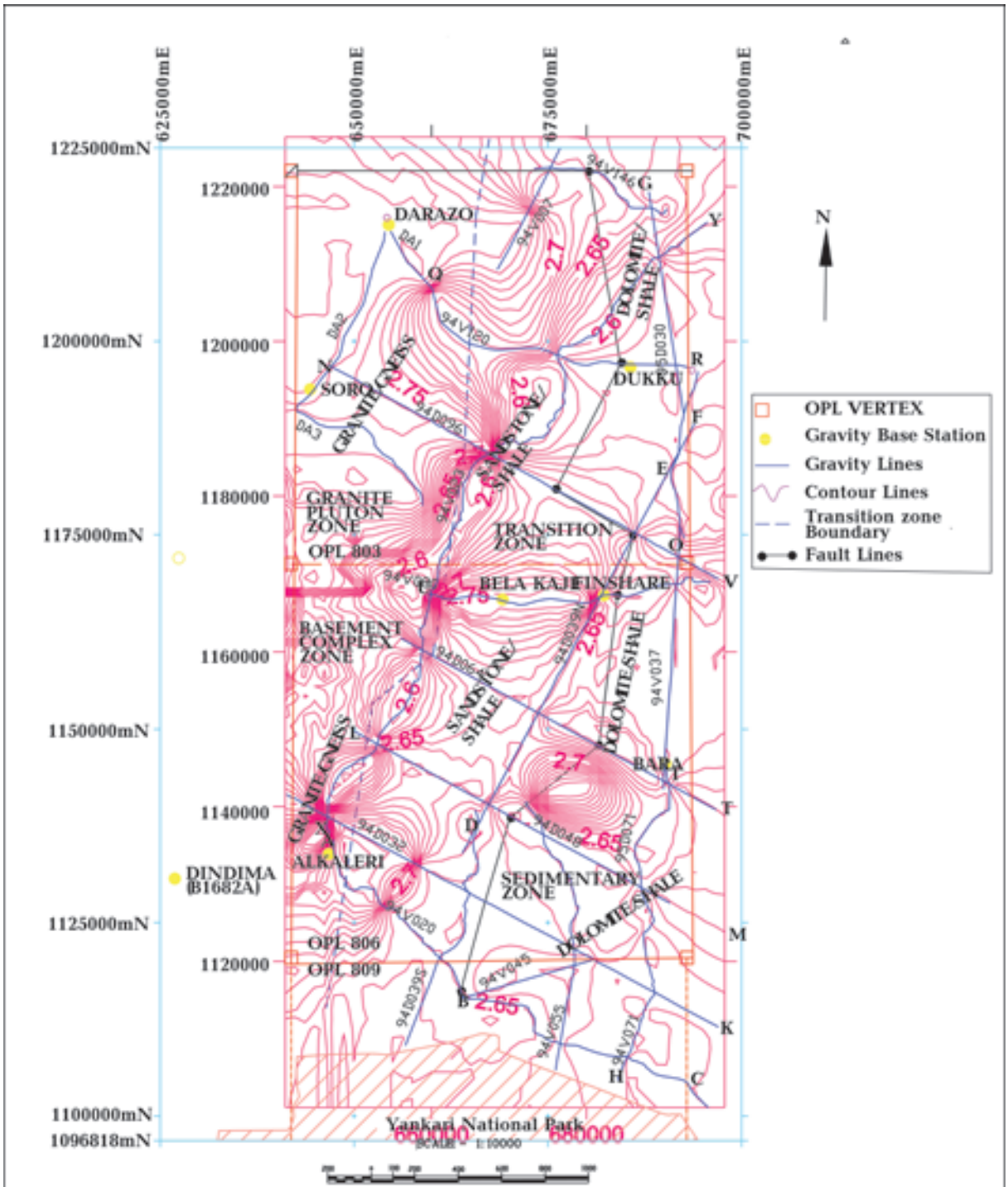


Fig. 10. Rock Density Map (C.I.=0,05 gcc).

Analysis of Results. Analysis of the Residual Gravity Profiles. From the fault parameters shown in Tabl. 2, it could be inferred that the limiting depth of the anomalous mass within this basin is between 152 m along line 94V020 and 469 m along line 94D096 profile. Also, the dip angle of the fault structures has its minimum value of 30° along line

94D032 profile and 70° along line 94V20 profile. The sediment thickness ranges from 1700 m in line 94D032 to 6500 m in line 94D096 respectively. The basement depth inferred from the above shows that the maximum depth of 7,0 km is obtained along line 94D096 and a minimum basement depth of 1900 m is obtained along 94D032 respectively.

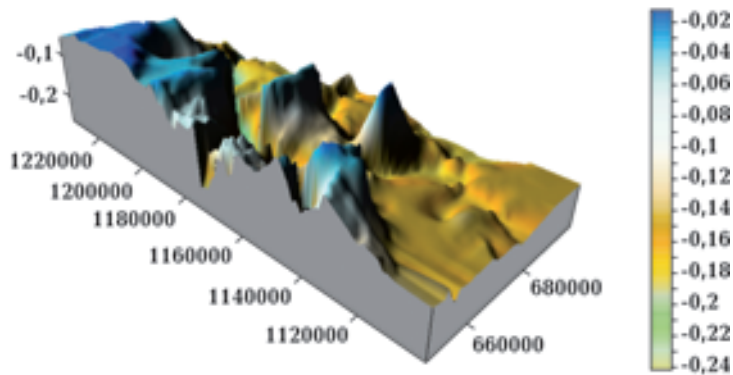


Fig. 9. 3D View of Basement Density Contrast.

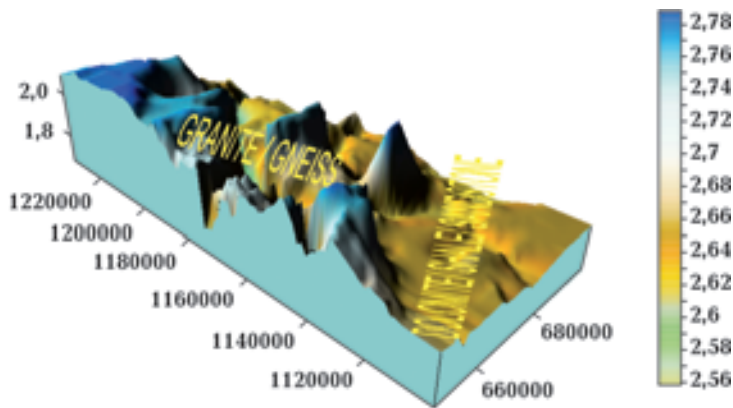


Fig. 11. 3D View of Rock Density Distribution.

Analysis of basement depth map. The basement depth map (Fig. 7) developed using the gravity data outlined the Gongola basin as a region of shallow and deep basement depths. The granite pluton and basement complex zone has a basement depth of between 1,9 km and 3,5 km respectively. The transition zone has a deep basement depth of between 3,5 km and 6,0 km, while the sedimentary zone has a deep basement depth of between 3,5 km and 7,0 km respectively.

Analysis of density contrast and rock density maps. Based on the computation of density contrast values using the step model approach, a density contrast map across the basin was produced. This is shown in Fig. 8. A 3D model of the density contrast map is shown in Fig. 9. Also, using the adopted density values for the rocks within the basin as shown in Tabl. 1, the rock density map with respect to the basement depth of the basin was produced. This is shown in Fig. 10 and 11 respectively.

From the maps, the following rock units were identified from the zones.

1. The sedimentary zone showed rock density values of 2,60 g/cc and 2,65 g/cc which showed the dominant presence of dolomite, shale and sandstone.
2. The transition zone showed the density values of 2,60g/cc, 2,65 g/cc and 2,70 g/cc in the Northern zone, which also showed the dominant presence of dolomite, shale, sandstone and granite. It also showed density values of 2,6g/cc, 2,65 g/cc and 2,7 g/cc in the southern part, which showed the dominant presence of dolomite, shale and sandstone and granite.
3. The granite pluton zone showed density values of 2,60 g/cc and 2,70 g/cc which showed the dominant presence of sandstone and granite.
4. The basement complex zone showed density values of 2,70 g/cc and 2,75 g/cc which showed the dominant presence of granite and gneiss.

Table 2. Step Model computation for faults dips, sediment thickness and basement density contrast

S/N	Line		K_1	K_2	D°	h/L	L , m	h , m	$\Delta\rho$, g/cm ³
1	94D032	A	1,25	1,33	30	0,07	1746	200	-0,04
		B	1,29	1,28	50	0,05	5898	295	0,15
2	94D039	A	1,25	1,36	32	0,10	1810	181	0,14
		B	1,20	1,30	42	0,07	4760	333	0,17
3	94D048	A	1,34	1,13	55	0,04	4813	193	0,14
		B	1,25	1,38	46	0,10	4440	444	0,16
4	94D064	A	1,32	1,36	40	0,05	3330	165	0,13
		B	1,25	1,33	60	0,1	4670	467	0,18
5	94D096	A	1,33	1,27	42	0,04	6010	312	0,04
		B	1,32	1,30	39	0,05	6500	469	0,13
6	94V020	A	1,27	1,30	45	0,05	3040	152	0,04
		B	1,20	1,23	70	0,01	5412	541	0,17
7	94V080	A	1,15	1,31	50	0,01	4075	407	0,04
		B	1,25	1,25	60	0,01	4332	433	0,18
8	94V120	A	1,21	1,28	42	0,05	4780	239	0,13
		B	1,25	1,26	50	0,05	4200	220	0,17
9	94V146	A	1,20	1,33	45	0,1	1800	180	0,12
		B	1,27	1,26	48	0,1	1700	170	0,11
10	Composite Line	A	1,18	1,35	52	0,10	4530	453	0,15
	94V071+95D071+94V037	B	1,22	1,34	59	0,10	4550	455	0,15
		C	1,25	1,28	52	0,10	4570	425	0,18

5. From the above description of the density distribution in the four zones, five rock contact boundaries of Dolomite, Shale, Sandstone, Granite and Gneiss were established based on their densities as shown in Table 1. It should be noted that the rock densities are not absolute values. There is always an overlap between the various rock densities.

Summary of Findings. The point of deflection on the residual gravity anomaly is isolated as a point of truncation of the fault plane and a change in density contrast.

1. Analysis of the residual anomaly profiles of the fault structures showed that the inversion of the fault structures were independent of the strike length.

2. The computed fault dips showed that the basement is segmented by normal faults.

3. The density contrast varies laterally due to fault truncations.

4. The inversion process simultaneously estimates the depth to basement. No initial depth input is required.

5. The basement depth map shows a region of shallow and deep basement ranging between 1,0 km in the basement complex zone and a maximum of 7,0 km in the north-eastern part of the sedimentary zone respectively.

6. The limiting depth of the anomalous mass ranges from 120 m to 541 m.

7. The rock density map determined from the density contrast map correlated with the geology of the basin.

Conclusion. It is observed in this research, that the step model inversion of residual gravity anomaly is an optimization procedure to estimate the four shape fault parameters. The application of the characteristic curves reduces the mathematical complexity observed in other methods

of gravity inversion. It is also observed that the Gongola basin basement is segmented by several northeast and northwest trending normal faults.

Acknowledgement. We thank Shell Nigeria Exploration and Production Company (SNEPCO) for the release of the data used in this research.

References

- Chakravarthi V.* Gravity Inversion of 2,5D faulted Beds Using Depth-Dependent Density // *Current Sci.* — 2008. — **95**, № 11. — P1618—1622.
- Dobrin M. B., Savit C. H.* Introduction to Geophysical Prospecting (4th Edition). — Singapore: McGrawHill Book Co., 1988. — 867 p.
- Grant F. S., West G. F.* Interpretation Theory In Applied Geophysics. — Toronto: McGrawhill Book Company, 1987. — 584 p.
- Keary P., Brooks M.* An Introduction to Geophysical Exploration. — London, 2002. — 294 p.
- Telford W. M., Geldart C. P., Sheriff R. T., Keys D. A.* Applied Geophysics. — Cambridge: University Press, 1990. — 852 p.